VNU Journal of Science: Mathematics – Physics, Vol. 38, No. 3 (2022) 49-61

VNU Journal of Science: Mathematics - Physics

Journal homepage: https://js.vnu.edu.vn/MaP

Original Article

# Calculation of the Dynamic Responses of Rails Subjected to Moving Loads on Ballasted Railway Track

Tran Le Hung*, Nguyen Dinh Duc

*VNU University of Engineering and Technology, 144 Xuan Thuy, Cau Giay, Hanoi, Vietnam*

Received 11 March 2022
Revised 09 April 2022; Accepted 12 April 2022

**Abstract:** The dynamical responses of railway track has been carried out by different ways. In this work, by developing an analytical model for the ballasted railway track which includes two rails connected to the railway sleeper, a fast method to calculated the dynamic responses of the two rails is presented. The rail is modelled as the infinite beams posed on the periodically supports which are rested on a viscoelastic foundation. We consider the dynamic equation in the steady-state of rails subjected to the moving loads. By using Fourier transform together the periodically conditions, a relation between the reaction force and the beam displacement in the frequency domain has been demonstrated. Then, by performing this relation into the dynamic equation of sleeper laying on viscoelastic foundation, the dynamic responses of the two rails can be obtained with a help of Green's function. The numerical example demonstrates the effect of the support on the beam responses.

*Keywords:* Dynamic, Structure, Railway track, periodically supported beam, Euler-Bernoulli beam.

## 1. Introduction

The dynamic responses of the railway track are always one of most interested research domains. There are different types of track as: non- ballasted railway track, ballasted railway track. A lot of analytical models have been developed. The first idea to model the railway track is supposing an infinite beam posed on a linear or on-linear foundation [1-4]. However, this type of the model is not really near to the railway track configuration, which has the discrete supports. Therefore, another model is developed by modelling an infinite beam posed on a periodic support. Mead [5, 6] presents a model with elastic supports and harmonic loads. Metrikine et al., [7] and Belotserkovskiy [8] proposed a method to

* Corresponding author.
*E-mail address:* hungtl@vnu.edu.vn

https//doi.org/10.25073/2588-1124/vnumap.4707

calculate the beam responses subjected to a moving concentrated load with the help of a periodicity condition. Nordborg [9, 10] used a Floquet's theorem and Fourier transform to solve the vertical rail vibrations problem. By using the same method, Hoang et al., [11] developed a model which allows to obtain analytical the rail responses in time domain. This work has been carried out with the two beams models for the rail. Tran et al., [12] presented an analytical model to calculate the track responses with non-uniform foundation. The dynamic responses of railway sleeper have been investigated by Tran et al., [13, 14]. By using Fourier transform together Green's function, the sleeper responses are shown analytically in the frequency domain. In addition, a method to calculate the moving loads is presented by Tran et al., [15] with the help of an inverse problem.

By using the analytical model, a dynamic of rail has been investigated but there is no model to calculate the responses of two rails. Therefore, several researches are developed with the help of numerical model thatwell agrees with the analytical model. Yang et al., [16] developed a FEM model which is validated by the measurement in-situ. Recently, Xiao and Ren [17] used a 3D vehicle-track-bridge element to study a stability of the railway bridge subjected to a moving force. Moreover, to reduce the degrees of freedom, Tran et al., [18] studied the sleeper responses laying on a non-homogeneous foundation by coupling an analytical model and numerical method. The influence of the crack sleeper on a track response has been carried out by Gustavson and Gylltoft [19]. By using the same method, Ruiz et al., [20] calculated the track responses by an implicit iteration.

This work presents a model to calculate the dynamic responses of the two rails on the ballasted railway track. The rail and a sleeper are modelled as a Euler-Bernoulli beam. The governing formulation is presented in the Section 2. Firstly, a model of the rail posed on a periodic support is written with the help of delta Dirac distribution. By using Fourier transform and a periodic condition of the moving loads and structures, an equivalent system has been demonstrated at each support. In other word, a reaction force applied on the beam can be expressed in function of the beam displacement via two functions: equivalent stiffness and equivalent load. This result has been demonstrated by Hoang et al., [21]. Then, with the help of Green's function and Fourier transform for the dynamic equation of sleeper, another relation between the reaction force and the sleeper displacement is found. By performing this relation into the periodically supported beam model, the reaction forces can be calculated in the function of the track parameters. Hence, the dynamic responses of the two rails can be obtained analytically in the frequency domain. In the Section 3, numerical example shows the rail displacement, rail strain and reaction force by taking into account the track parameters of the railway track in Vietnam. A parametric study shows the influence of the distance between two blocks on the rail responses. Finally, concluding remarks are drawn in the Section 4.

## 2. Formulation

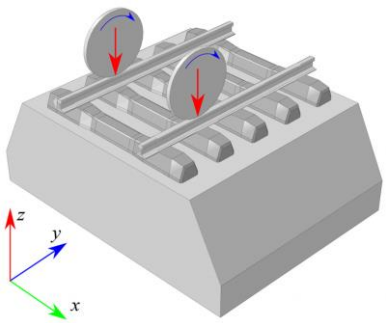


Figure 1. Ballasted railway track.

Let us consider that the railway ballasted track can be modelled as shown in Figure 1. In this figure, the railway track contains two rails, supports of the rail and foundation.

*2.1. Periodically Supported Beam Model and Equivalent System*

In the $Oyz$ plan, a rail is modelled by the periodically supported beam model as shown in Figure (2). In this figure, all supports are separated by a distance $l$. The rail is subjected to the $K$ moving loads $Q_j$ (with $1 \leq j \leq K$) which is defined by a distance $D_j$ to the first wheel. With the help of the Dirac distribution and by considering that the moving loads are the concentrated loads on the beam, the sum of moving loads can be detailed as follow:

$$Q_j = \sum_{j=1}^{K} Q_j \delta(y + D_j - vt) \tag{1}$$

where $v$ is the train speed.

In addition, let $R_n$ be the reaction force of the support $n$ applied to the rail as shown in Figure 2. This force can be expressed with the help of Dirac distribution at the coordinate $y = nl$ (with $n \in \mathbb{Z}$). Moreover, in steady-state condition, we suppose that all supports are equivalent and their responses can be described by the same way, but with a time delay which is calculated by the time the moving loads travel from one support to another. In other word, this assumption can be explained by: $R_n(t) = R\left(t - \frac{nl}{v}\right)$ where $R(t)$ is the reaction force of the support at $y = 0$. Hence, sum of the reaction forces $R_s(t)$ applied to the beam can be expressed as follows:

$$R_s(t) = \sum_{n=-\infty}^{\infty} R_n \delta(y - nl) = \sum_{n=-\infty}^{\infty} R\left(t - \frac{y}{v}\right) \delta(y - nl) \tag{2}$$

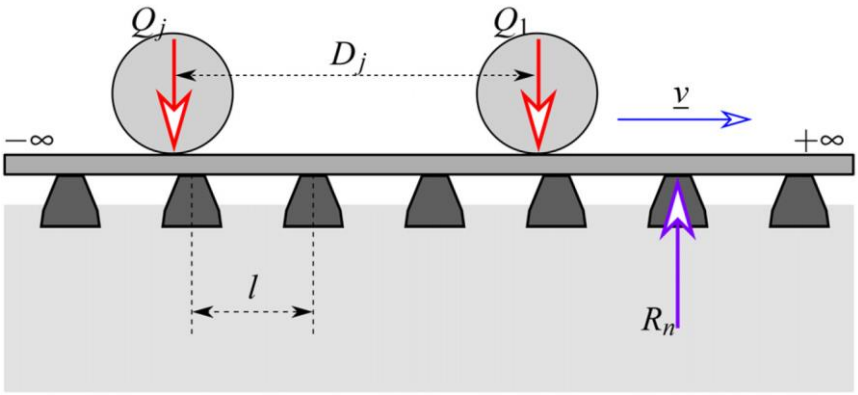


Figure 2. Periodically supported beam model for the rail.

By substituting Eq. (1) and Eq. (2), the total force applied on the rail is the following result:

$$F(y,t) = \sum_{n=-\infty}^{\infty} R\left(t - \frac{y}{v}\right) \delta(y - nl) - \sum_{j=1}^{K} Q_j \delta(y + D_j - vt) \tag{3}$$

The rail can be modelled as a Euler-Bernoulli beam, so the dynamic equation is written as:

$$E_r I_r w_r''''(y,t) + \rho_r S_r \ddot{w}_r(y,t) = F(y,t) \tag{4}$$

where $E_r$, $\rho_r$, $S_r$ and $I_r$ are Young's modulus, density, section and second moment of area of the beam respectively. The notations $(\blacksquare)'$ and $(\dot{\blacksquare})$ stand for the partial derivative with regard to $y$ and to time $t$. By using the Fourier transform of the last equation two times and then inverse Fourier transform, we can obtain the relation between the displacement of the support and the reaction force in the frequency domain: (see Hoang et al. [20]):

$$\widehat{\boldsymbol{R}}(\omega) = \mathcal{K}(\omega)\widehat{\boldsymbol{w}}_{\boldsymbol{r}}(\omega) + \mathcal{Q}(\omega) \tag{5}$$

where two functions $\mathcal{K}(\omega)$ and $\mathcal{Q}(\omega)$ are equivalent stifness and equivalent loads respectively which are defined as follows:

$$\begin{cases} \mathcal{K}(\omega) = 4\lambda_r^3 E_r I_r \left[ \dfrac{\sin \lambda_r l}{\cos \lambda_r l - \cos \dfrac{\omega}{v} l} - \dfrac{\sinh \lambda_r l}{\cosh \lambda_r l - \cos \dfrac{\omega}{v} l} \right]^{-1} \\ \mathcal{Q}(\omega) = \mathcal{K}(\omega) \displaystyle\sum_{j=0}^{K} \dfrac{Q_j e^{-i\frac{\omega}{v} D_j}}{v E_r I_r \left[ \left(\dfrac{\omega}{v}\right)^4 - \lambda_r^4 \right]} \end{cases} \tag{6}$$

where $\lambda_r = \sqrt[4]{\dfrac{\rho_r S_r \omega^2}{E_r I_r}}$. Eq. (6) describes a relation between the reaction force applied to the support and the rail displacement. So, the equivalent system can be presented as shown in Figure 3.

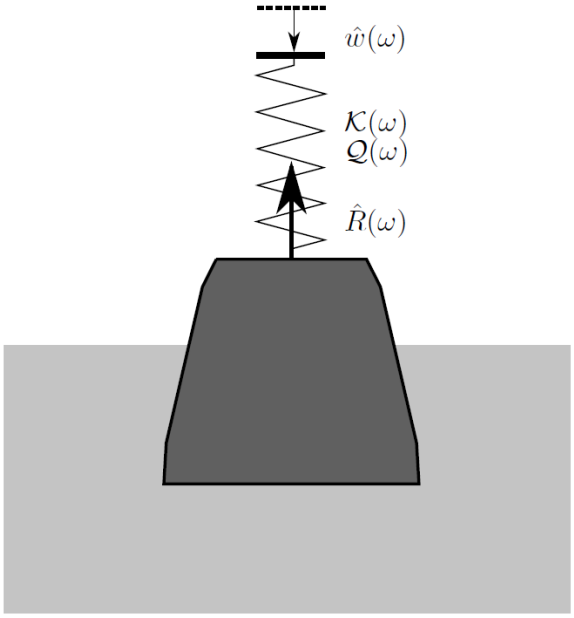


Figure 3. Equivalent system in the frequency domain.

In this system, the equivalent stiffness and equivalent loads do not depend on the parameters of support. Two functions depend on the parameters of beam are the railway track and the moving loads. Thus, this equation can be used for all of the type of supports, as linear or non-linear supports. In addition, the dynamic responses of rail can be obtained in the frequency domain as follows:

$$\widehat{w}_r(y,\omega) = \hat{R}(\omega)\,\eta(y,\omega) - Q(\omega)\,\eta_0(\omega)e^{-i\frac{\omega}{v}y} \tag{7}$$

where:

$$\begin{cases} \eta(y,\omega) = \dfrac{1}{4\lambda_r^3 E_r I_r}\left[\dfrac{\sin\lambda_r(l-y) + e^{-i\frac{\omega l}{v}}\sin\lambda_r y}{\cos l\lambda_r - \cos\frac{\omega l}{v}} - \dfrac{\sinh\lambda_r(l-y) + e^{-i\frac{\omega l}{v}}\sinh\lambda_r y}{\cosh l\lambda_r - \cos\frac{\omega l}{v}}\right] \\ \eta_0(\omega) = \eta(0,\omega) = \dfrac{1}{4\lambda_r E_r I_r}\left[\dfrac{\sin\lambda_r l}{\cos l\lambda_r - \cos\frac{\omega l}{v}} - \dfrac{\sinh\lambda_r l}{\cosh l\lambda_r - \cos\frac{\omega l}{v}}\right] \end{cases} \tag{8}$$

*2.2. Analytical Model of the Railway Ballasted Track*

In the ballasted railway track, the two rails are supported by the mono-block sleeper which is posed on the foundation as shown in Figure 4.

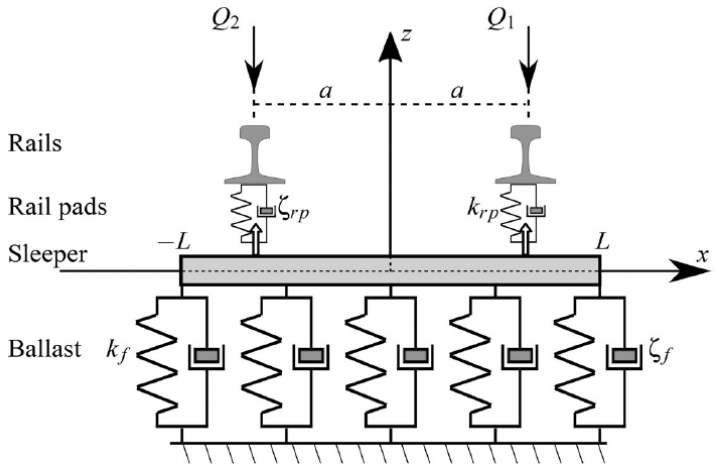


Figure 4. Model of railway sleeper laying on viscoelastic foundation.

In this figure, the sleeper is presented as a Euler-Bernoulli beam that the length is $2L$ (with $-L \leq x \leq L$) and the rails positions are $x = \pm a$. The ballast can be modelled as a viscoelastic foundation which is characterized by the stiffness $k_f$ and damping $\zeta_f$. At the contacts rail-sleeper, in order to reduce the impact of the rail's vibration and to protect the supports, the engineers use the rail-pads which are made by rubber. In this model, we modelled it by using the spring-damper system as shown in Figure 4 which is characterized by stiffness $k_{rp}$ and damping $\zeta_{rp}$. The dynamic equation of the beam can be written as:

$$E_s I_s w_s''''(x,t) + \rho_s S_s\,\ddot{w}_s(x,t) + k_b w_s(x,t) + \zeta_b \dot{w}_s(x,t) = -R_1(t)\delta(x-a) - R_2(t)\delta(x+a) \tag{9}$$

where $R_1$ and $R_2$ are two reaction forces applied on the beam. The parameters $E_s$, $I_s$, $\rho_s$ and $S_s$ are the Young's modulus, second moment of area, density and section of the sleeper respectively. By using the Fourier transform, Eq. (9) is rewritten in the frequency domain as follow:

$$\widehat{w}_s''''(x,\omega) - \left(\frac{\rho_s S_s \omega^2 - k_f}{E_s I_s}\right)\widehat{w}_s(x,\omega) = \frac{-\hat{R}_1(\omega)}{E_s I_s}\delta(x-a) + \frac{-\hat{R}_2(\omega)}{E_s I_s}\delta(x+a) \tag{10}$$

where $k_b = k_f + i\omega\zeta_f$ is the dynamic stiffness of foundation. Eq. (10) presents a linear differential equation order 4 which the solution can be found with the help of Green's function:

$$\widehat{w}_s(x,\omega) = \frac{-\hat{R}_1(\omega)}{E_s I_s}G(x,\omega;a) + \frac{-\hat{R}_2(\omega)}{E_s I_s}G(x,\omega;-a) \tag{11}$$

where is the Green's function which is defined as follows (see Tran et al. [23]):

$$G(x,\omega;a) = \begin{cases} A_1\cos\lambda_s x + A_2\sin\lambda_s x + A_3\cosh\lambda_s x + A_4\sinh\lambda_s x \;\; for\; x \in [-L,a] \\ B_1\cos\lambda_s x + B_2\sin\lambda_s x + B_3\cosh\lambda_s x + B_4\sinh\lambda_s x \;\; for \;\; x \in [a,L] \end{cases} \tag{12}$$

where $\lambda_s = \sqrt[4]{\frac{\rho_s S_s \omega^2 - k_b}{E_s I_s}}$. Eq. (11) allows us to calculate the dynamic responses of the sleeper in the frequency domain when the two reaction forces are determined.

*2.3. Solution of the Problem*

The sleeper displacements at the contacts rail-sleeper are calculated with the help of Eq. (11) as follow:

$$\begin{cases} \widehat{w}_s(a,\omega) = \dfrac{-\hat{R}_1(\omega)}{E_s I_s}G(a,\omega;a) + \dfrac{-\hat{R}_2(\omega)}{E_s I_s}G(a,\omega;-a) \\ \widehat{w}_s(-a,\omega) = \dfrac{-\hat{R}_1(\omega)}{E_s I_s}G(-a,\omega;a) + \dfrac{-\hat{R}_2(\omega)}{E_s I_s}G(-a,\omega;-a) \end{cases} \tag{13}$$

By using the consecutive law of the rail-pads, the reaction force can be expressed in other way:

$$\begin{cases} \hat{R}_1(\omega) = -k_p\left[\widehat{w}_r^{[1]}(\omega;a) - \widehat{w}_s(a,\omega)\right] \\ \hat{R}_2(\omega) = -k_p\left[\widehat{w}_r^{[2]}(\omega;-a) - \widehat{w}_s(-a,\omega)\right] \end{cases} \tag{14}$$

where $k_p = k_{rp} + i\omega\zeta_{rp}$ is the dynamic stiffness of the rail pad, and are the displacement the two rails at the contact rail-sleeper. The notations $\widehat{w}_r^{[1]}(\omega;a)$, $\widehat{w}_r^{[2]}(\omega;-a)$ are the displacements of the rail 1 and 2 respectively at the contact with the support. Hence, by performing Eqs. (5), (13) and (14), the reaction forces applied on the sleeper can be calculated as follows:

$$\begin{cases} \hat{R}_1(\omega) = \dfrac{E_s I_s}{\mathcal{K}}\dfrac{Q_1[G(-a,\omega;-a)+\chi] - Q_2 G(a,\omega;-a)}{\widetilde{D}} = \tilde{A}_1 Q_1 + \tilde{B}_1 Q_2 \\ \hat{R}_2(\omega) = \dfrac{E_s I_s}{\mathcal{K}}\dfrac{Q_2[G(a,\omega;a)+\chi] - Q_1 G(-a,\omega;a)}{\widetilde{D}} = \tilde{B}_2 Q_1 + \tilde{A}_2 Q_2 \end{cases} \tag{15}$$

where:

$$\begin{cases} \widetilde{D} = [\chi + G(a,\omega;a)][\chi + G(-a,\omega;-a)] - G(a,\omega;-a)G(-a,\omega;a) \\ \chi = E_s I_s\left(\dfrac{k_f \mathcal{K}}{k_f + \mathcal{K}}\right) \end{cases} \tag{16}$$

By performing Eq. (15) into Eq. (7), the dynamic responses of the two rails are obtained as follows:

$$\begin{cases} \widehat{w}_r^{[1]}(y,\omega) = -\left[\eta_0(\omega)e^{-i\frac{\omega}{v}y} - \tilde{A}_1\eta(y,\omega)\right] Q_1 + \tilde{B}_1\eta(y,\omega)Q_2 \\ \widehat{w}_r^{[2]}(y,\omega) = -\left[\eta_0(\omega)e^{-i\frac{\omega}{v}y} - \tilde{A}_2\eta(y,\omega)\right] Q_2 + \tilde{B}_2\eta(y,\omega)Q_1 \end{cases} \quad (17)$$

Moreover, the rail strain in the frequency domain can be obtained as follows:

$$\hat{\varepsilon}_{xx}^{[j]}(y,\omega) = \mathcal{F}\left(-z\left(w_r^{[k]}(y,\omega)\right)''\right) = z\omega^2\widehat{w}_r^{[j]}(y,\omega) \quad (18)$$

where $\hat{\varepsilon}_{xx}^{[j]}$ is the rail strain at the rail $j$ (with $j = 1,2$) and $\mathcal{F}(\blacksquare)$ stands for the Fourier transform.

*Remark:* By replacing $x = 0$ into Eq. (17), we can get the displacement of the two rails at the support:

$$\begin{cases} \widehat{w}_r^{[1]}(0,\omega) = -\left[1 - \tilde{A}_1\right]\eta_0(\omega)\, Q_1 + \tilde{B}_1\eta_0(\omega)Q_2 \\ \widehat{w}_r^{[2]}(0,\omega) = -\left[1 - \tilde{A}_2\right]\eta_0(\omega)\, Q_2 + \tilde{B}_2\eta_0(\omega)Q_1 \end{cases} \quad (19)$$

To conclude, in this section, by coupling the periodically supported beam model and the dynamic model of the sleeper, the dynamic responses of the two rails are expressed in the frequency domain as shown in the Eqs. (17) and (18). The solution of the problem can be presented in the time domain by using the invers Fourier transform.

## 3. Results and Discussion

### *3.1. Validation of the Present Study*

In order to validate this model, we will compare the rail displacement at the support and the reaction force with the ones calculated by analytical model developed by Hoang et al., [20]. In his work, the track responses can be calculated analytically in the time domain.

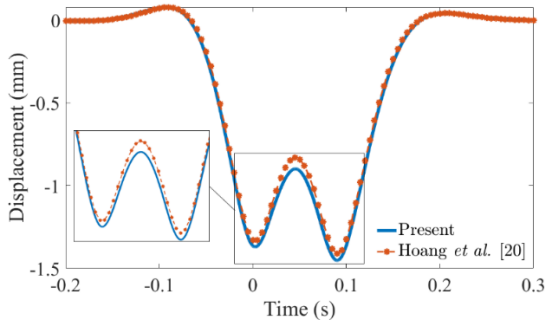


Figure 5. Comparison of the rail displacement.

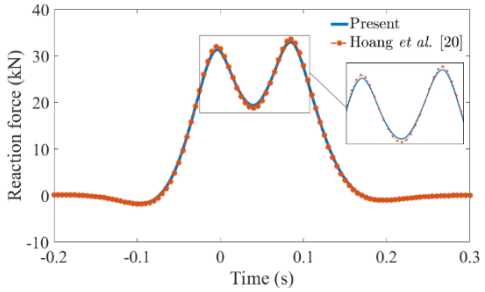


Figure 6. Comparison of the reaction force.

The results obtained by this model is calculated in the symmetric configuration (homogeneous foundation, two moving loads are equal and two rails have the same mechanical parameters). Hence, the responses on the two rails are obviously the same. All track parameters used are the same as the study of Hoang et al., [21]. The comparisons of the displacement and the reaction force are shown in Figures 5 and 6. In these figures, continuous blue line presents the results calculated by this model and the discontinuous red dotted line stands for the ones obtained by Hoang et al.

A maximum difference of the rail displacement obtained at the moment between the two-wheel loads pass on the sleeper and this value is 7.78 %. The difference of rail displacement when the two-wheel loads passes is 2.76 %. The difference of reaction force is 2.56%. Hence, we can conclude that there is a small difference between the results obtained in this paper and those determined in existing publication.

### *3.2. Numerical Example*

In this section, we present here a numerical example of the dynamic model by considering all of the track parameters are shown in the Table 1. The track parameters accord to the railway track in Vietnam. In this example, we present the dynamic responses of the two rails with the passing of one wagon, which contains 4 axles. The 8 moving loads are shown in the Table 2. According to this table, we see that the moving loads at the rail 1 are identical: meanwhile in the rail 2, the 3rd wheel applied a higher load than the others. This simulation corresponds to the case of wheel default or overload. The train velocity is 75 $kmh^{-1}$, corresponding to the average speed of train in Vietnam.

Table 1. Railway track parameters [21]

| Content | Notation | Unit | Value |
|---|---|---|---|
| Young's modulus of rail | $E_r$ | GPa | 210 |
| Second moment of inertia of rail | $I_r$ | $m^4$ | $3 \times 10^{-5}$ |
| Rail density | $\rho_r$ | $kgm^{-3}$ | 7850 |
| Rail section area | $S_r$ | $m^2$ | $7.69 \times 10^{-3}$ |
| Young's modulus of sleeper | $E_s$ | GPa | 40 |
| Second moment of inertia of sleeper | $I_s$ | $m^4$ | $1.24 \times 10^{-4}$ |
| Sleeper density | $\rho_s$ | $kgm^{-3}$ | 2500 |
| Sleeper section area | $S_s$ | $m^2$ | $30.8 \times 10^{-3}$ |
| Length of sleeper | $2L$ | m | 1.8 |
| Track gauge | $2a$ | m | 1.0 |
| Sleeper spacing | $l$ | m | 0.6 |
| Stiffness of foundation | $k_b$ | $MNm^{-1}$ | 240 |
| Damping coefficient of foundation | $\zeta_b$ | $kNsm^{-1}$ | 58.8 |
| Stiffness of rail pad | $k_{rp}$ | $MNm^{-1}$ | 192 |
| Damping coefficient of rail pad | $\zeta_{rp}$ | $MNsm^{-1}$ | 1.97 |

Table 2. Moving loads parameters

| | Axle 1 | Axle 2 | Axle 3 | Axle 4 |
|---|---|---|---|---|
| Rail 1 | 100 kN | 100 kN | 100 kN | 100 kN |
| Rail 2 | 100 kN | 100 kN | 125 kN | 100 kN |

Figure 7 presents a reaction forces apply on two rails at the support, by taking the reference time $t = 0$ when the first wheel passes. The dynamic responses applied on the rail 1 and 2 are colored by the

blue and red lines respectively. The reaction forces applied on the two rails when the two first axles passe are equal (47.87 kN). When the third axle passes, the rail 2 is subjected a bigger reaction force (60.12 kN) while reaction force applied on the rail 1 is the same (47.87 kN). This phenomenon affects on the dynamic sleeper responses which have been demonstrated by Tran et al., [12]. When the fourth axle passes, the rail 2 is subjected a reaction force which is slightly smaller than the one applied on the rail 1 (47.57 kN compare with 47.87 kN) even though the train loads are the same.

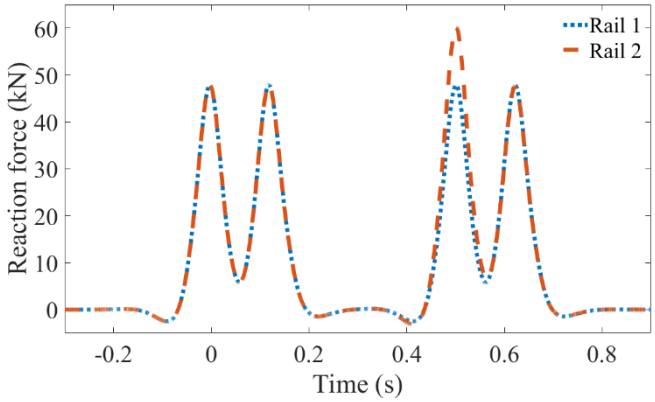


Figure 7. Reaction force applied on the two rails.

The displacements of the two rails are shown in Figure 8. When the moving loads applied on the two rails are identical, the rail displacements are the equal (0.45 mm). The rail displacement on the rail 2 is bigger than the one on the rail 1 when third wheel passes (0.57 mm to compare with 0.45 mm). The displacements of the two rails accord to the reaction force applied in case of homogeneous foundation.

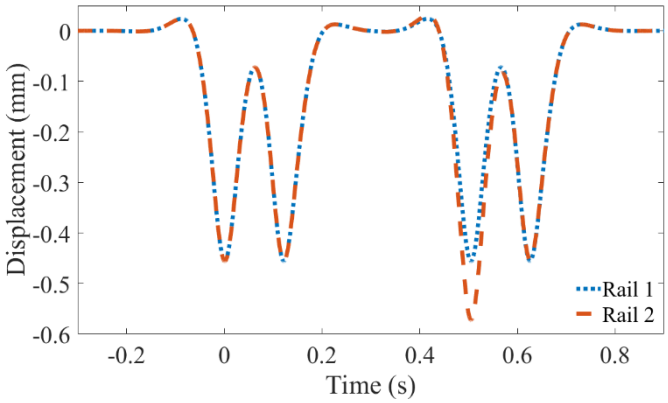


Figure 8. Displacement of the two rails at the support $y = 0$.

Now, we present here, in Figure 9, a rail displacement at the support and the middle between the two support by taking into account the condition of symmetric moving loads (the rail loads are identical at two rails: $Q_j^{[1]} = Q_j^{[2]} = 100$ kN). Hence, the responses of the two rails are obviously symmetric (see Figure 8). Therefore, Figure 9 shows only the displacement of one rail inspire of two. We see that the rail displacement at the middle of two supports (dotted line) is higher than the one at the support (continuous line) about 4.5%.

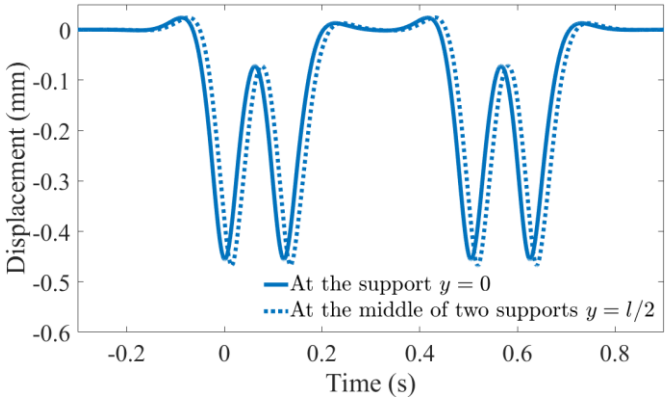


Figure 9. Displacement of rail at the support position (continuous line) and at the middle between two support (dotted line).

The strain of the rail at the two positions ($y = 0$ and $y = l/2$ ) is shown in Figure 10. At the block position, the rail deforms less when we compare with the middle of the two supports position (0.025 to compare with 0.034, about 36%). This phenomenon demonstrates the influence of the support on the rail. Moreover, the appearance of peaks in the rail strain can be explained by the fact that we used the Dirac distribution to describe the reaction force $R_n$ (see Eq. 2)

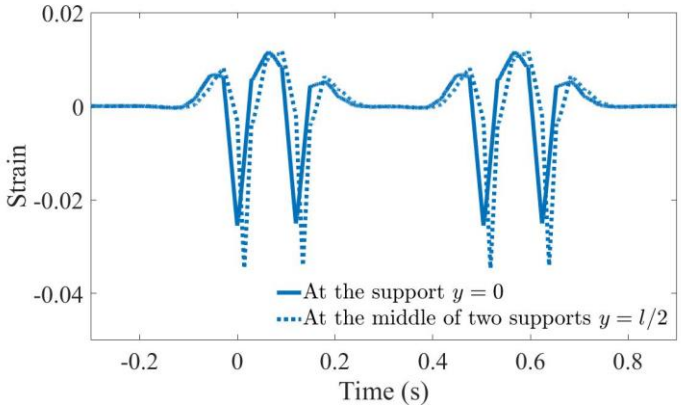


Figure 10. Strain of rail at the support position (continuous line) and at the middle between two support (dotted line).

### *3.3. Parametric Studies*

In this section, a parametric study has been carried out to study the distance between two supports on the rail displacement. In order to simplify the result, the dynamic responses of the rails have been calculated by only one moving loads and symmetric loads. Figure 11. In this figure, the rail displacement is calculated in 4 cases: $l = 0.2$ m (red line), $l = 0.6$ m (black line), $l = 1.0$ m (yellow line) and $l = 1.4$ m (green line). Figure 11 shows the results at the block position $y = 0$ (marker circle) and at the middle between two blocks $y = l/2$ (marker star). When the distance between two blocks is small, the rail is well supported, thus the displacement is small. More this distance is large, more the rail displacement is big. The difference between the maximum of rail displacement is shown in Figure 12.

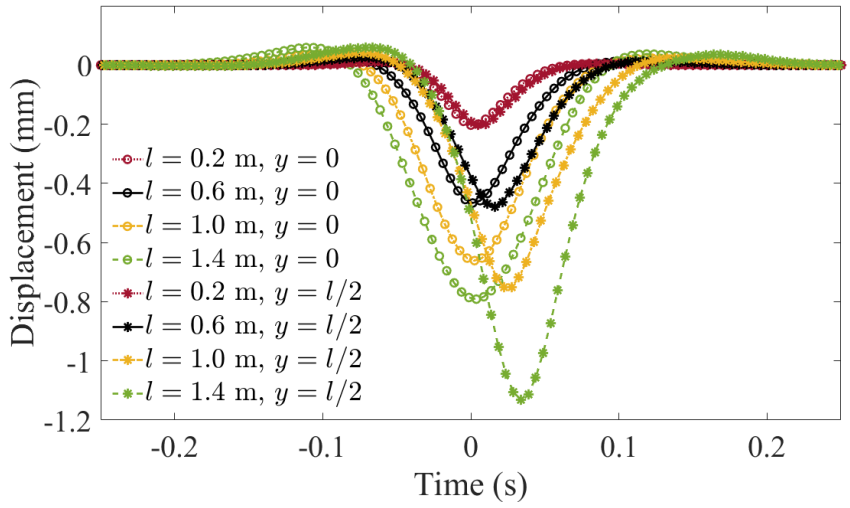


Figure 11. Influence of the distance between two blocks on the rail displacement at two positions.

Figure 12 shows the maximum displacement of the rail at two positions: at the support (dotted blue line with circle marker) and at the middle of the two blocks (continuous blue line and marker star) in the function of the distance between the two blocks. The difference between the two values is presented by the red line with marker square. The difference increases with the increase of the distance. For the safety caution, the railway track could not be constructed with a large distance between two supports. Besides, when this distance is small, the rail is absolutely well supported. However, this configuration creates a financial problem. This study demonstrates the choice of the distance between two supports in the norms.

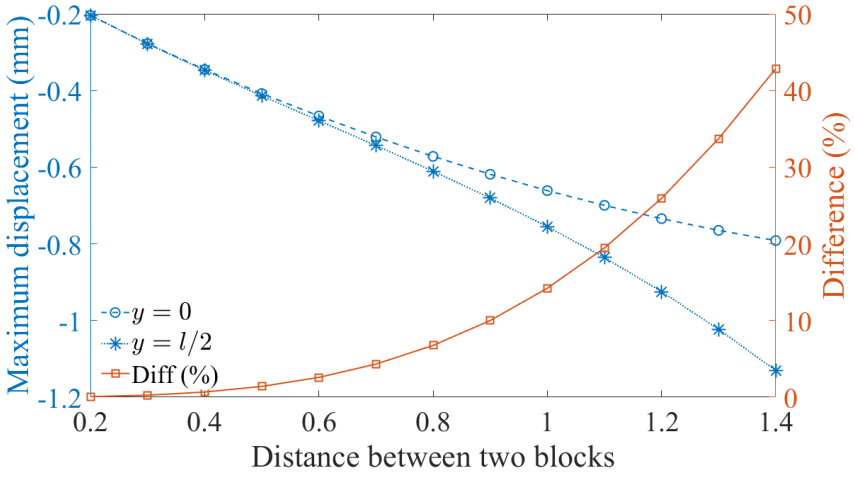


Figure 12. Difference of the maximum rail displacement at two positions in function of the distance between two supports.

## 4. Conclusion

In this work, an analytical model for the dynamic responses of rails on ballasted railway track is developed. By considering the rail as the infinite beam on a periodically supports, a relation between the reaction force applied on the rail and rail displacement in the frequency domain has been demonstrated. Then, Euler-Bernoulli equation has been written for the mono block sleeper laying on a visco-elastic foundation, the dynamic response of the sleeper was calculated with the help of Green's function. By coupling the two models, the reaction force and the displacement of the rails were calculated analytically in the frequency domain. There is a little difference between the results obtained by this model and the ones that were reported in published works. The numerical examples have showed the displacement of the two rails. The influence of the distance between two blocks was shown in the parametric studies. The advantage of this model shows that one can use it to calculate the dynamic responses of two rails, whereas by the other models one can obtain the responses for only one rail. In further works, this model can be developed by using Timoshenko beam model combined with experimental measurements.

## Acknowledgments

This work has been supported by VNU University of Engineering and technology under project number CN21.22.

## References

[1] L. Frýba, Vibration of Solids and Structures Under Moving Load, 3rd edition, Research Institute of Transport, Thomas Telford, 1972.

[2] V. H. Nguyen, D. Duhamel, Finite Element Procedures for Nonlinear Structure in Moving Coordinates – Part 1: Infinite Bar Under Moving Axial Loads, Computer and Structures, Vol. 84, 2006, https://doi.org/10.1016/j.compstruc.2006.02.018.

[3] V. H. Nguyen, D. Duhamel, Finite Element Procedures for Nonlinear Structure in Moving Coordinates – Part 2: Infinite Bar Under Moving Harmonic Loads, Computer and Structures, Vol. 86, 2008, https://doi.org/10.1016/j.compstruc.2008.04.010.

[4] T. Hoang et al., Respone of a Periodically Supported Beam on a Nonlinear Foundation Subjected to Moving Loads, Nonlinear Dynamic, Vol. 86, 2016, https://doi.org/10.1007/s11071-016-2936-5.

[5] D. Mead, Free Wave Propagation in Periodically Supported, Infinite Beam, Journal of Sound and Vibration, Vol. 11, 1970, https://doi.org/10.1016/S0022-460X(70)80062-1.

[6] D. Mead, Wave Propagation in Continuous Periodic Structures: Research Contributions from Southampton: 1964-1965, Journal of Sound and Vibration, Vol. 190, 1996, https://doi.org/10.1006/jsvi.1996.0076.

[7] A. V. Metrikine, Vibration of a Periodically Supported Beam on an Elastic Half-space, European Journal of Mechanic - A/Solid, Vol. 18, 1999, https://doi.org/10.1016/S0997-7538(99)00141-2.

[8] P. M. Belotserkovskiy, On the Oscillations of Infinite Periodic Beams Subjected to a Moving Concentrated Force, Journal of Sound and Vibration, Vol. 196, 1996, https://doi.org/10.1006/jsvi.1996.0309.

[9] A. Nordborg, Vertical Rail Vibrations: Pointforce Excitation, Acta Acustica Vol. 84, 1998.

[10] A. Nordborg, Vertical Rail Vibrations: Parametric Excitation, Acta Acustica, Vol. 84, 1998.

[11] T. Hoang et al., Dynamical Response of a Timoshenko Beams on a Periodical Nonlinear Support Subjected to Moving Forces, Engineering Structures, Vol. 176, 2018, https://doi.org/10.1016/j.engstruct.2018.09.028.

[12] L. H. Tran et al., Calculation of the Dynamic Responses of a Railway Track on a Non-uniform Foundation, Journal of Vibration and Control, 2022, https://doi.org/10.1177/10775463221099353.

[13] L. H. Tran et al., A Fast Analytic Method to Calculate the Dynamic Response of Railway Sleeper, Journal of Vibiration and. Acoustic, Vol. 141, 2019, https://doi.org/10.1115/1.4040392.

[14] L. H. Tran et al., A Comparison of Beam Models for the Dynamics Responses of Railway Sleepers, International Journal of Rail and Transportation, Vol. 10, 2022, https://doi.org/10.1080/23248378.2022.2034062.

[15] L. H. Tran et al., Identification of Train Loads from the Dynamic Responses of an Integrated Sleeper in Situ, Journal of Intelligent Material Systems and Structures, Vol. 31, 2020, https://doi.org/10.1177/1045389X20922905.

[16] X. Yang et al., An Explicit Periodic Nonlinear Model for Evaluating Dynamic Responses of Damaged Slab Track Involving Material Nonlinearity of Damage in High-speed Railway, Construction and Building Materials, Vol. 168, 2018, https://doi.org/10.1016/j.conbuildmat.2018.02.147.

[17] X. Xiao, W. X. Ren, A Versatile 3D Vehicule-track-bridge Element for Dynamics Analysis of Railway Bridges Under Moving Train Loads, International Journal of Structural Stability and Dynamics, Vol. 19, 2019, https://doi.org/10.1142/S0219455419500500.

[18] L. H. Tran et al., Influence of Non-homogeneous Foundation on the Dynamic Responses of Railway Sleepers, International Journal of Structural Stability and Dynamics, Vol. 21, 2020. https://doi.org/10.1142/S0219455421500024.

[19] R. Gustavson, K. Gylltoft, Influence of Cracked Sleepers on the Global Track Responses: Coupling of a Linear Track Model and Nonlinear Finite Element Analyses, Proceedings of the Institution of Mechanical Engineers, Part F: Journal of Rail and Rapid Transit, Vol. 216, 2002, https://doi.org/10.1243/0954409021531674.

[20] J. F. Ruiz et al., Study of Ground Vibrations Induced by Railway Traffic in a 3D FEM Model Formulated in the Time Domain: Experimental Validation, Structure and Infrastructure Engineering, Vol. 13, 2017, https://doi.org/10.1080/15732479.2016.1172649.

[21] T. Hoang et al., Calculation of Force Distribution for a Periodically Supported Beam Subjected to Moving Loads, Journal of Sound and Vibration, Vol. 388, 2017, https://doi.org/10.1016/j.jsv.2016.10.031.

[22] Vietnam Building codes on railway TCCS 04:2014/VNRA, http://vnra.gov.vn/Media/AuflaNews/Attachment/TCCS.04.2014.VNRA.30.12.2014.pdf, 2014 (acces on: March 8th, 2022).

[23] L. H. Tran et al., Analytical Model of the Dynamics of Railway Sleeper, presented at 6th International Conference on Computational Methods in Structural Dynamics and Earthquake Engineering, Rhodes Island, Greece, 2017, https://doi.org/10.7712/120117.5695.18372.